

pubs.acs.org/acsapm Article

# Triazine- and Heptazine-Based Porous Organic Polymer Networks for the Efficient Removal of Perfluorooctanoic Acid

Dana Abdullatif, Ahmadreza Khosropour, Anahita Khojastegi, Imann Mosleh, Leila Khazdooz, Amin Zarei, and Alireza Abbaspourrad\*



Cite This: ACS Appl. Polym. Mater. 2023, 5, 412-419



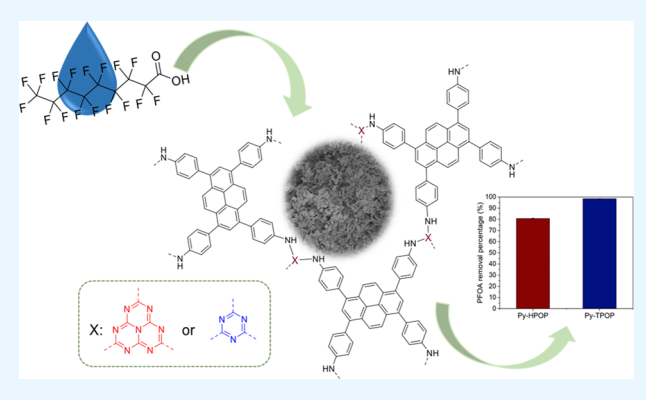
**ACCESS** 

III Metrics & More

Article Recommendations

s Supporting Information

ABSTRACT: The presence of perfluorooctanoic acid, a perfluoralkyl substance, in water sources has raised health concerns due to its toxicity. Finding effective adsorbents is essential to ensure healthy sources of water for consumption. In this study, a heptazine-based polymer network (Py-HPOP) was synthesized using a one-pot nucleophilic substitution of 2,5,8-trichloro-s-heptazine (TCH) with 4,4′,4″,4‴-(pyrene-1,3,6,8-tetrayl) tetraaniline (Py-TA). For comparison, a triazine-based polymeric network (Py-TPOP) was also prepared using 2,4,6-trichloro-1,3,5-triazine under similar conditions. Both polymers were used to treat aqueous solutions containing 1 mg/L PFOA. Py-TPOP exhibited superior adsorption capacity (98.4% PFOA removal) relative to Py-HPOP (80.8% PFOA removal) despite Py-HPOP's higher Brunauer—Emmett—Teller (BET) surface area



 $S_{\rm BET}$  at 205 m<sup>2</sup> g<sup>-1</sup>. The effect of electrostatic interactions was also observed as a critical factor for PFOA adsorption as demonstrated by the change in PFOA adsorption by both polymers under basic, neutral, and acidic conditions. This investigation illustrates a facile synthesis of amorphous covalent frameworks as strong, competitive adsorbents for PFOA removal from water.

KEYWORDS: perfluoroalkyl substance, perfluorooctanoic acid, triazine, heptazine, porous organic polymer

#### INTRODUCTION

Water quality and safety are increasingly regulated to ensure healthy consumption. Among various pollutants of concern are per- and polyfluoroalkyl substances (PFAS), a class of organic substances with partially or fully fluorinated alkyl chains terminated by various functionalities, most commonly sulfonic, phosphonic, and carboxylic acids. 1-3 Due to the strong C-F bonds present, they are widely used for their resistance to degradation in applications, including fibers and textiles, packaging materials, and waterproof/nonstick coatings.<sup>2,4</sup> Some of the most heavily produced PFAS, such as perfluorooctanoic acid (PFOA), are water soluble and linked to health hazards such as cancer and adverse reproductive effects. 5,6 Therefore, safe, efficient methods for the removal of PFAS from water are needed. While adsorption using activated carbon is a widely used method because it is inexpensive and environmentally friendly, these adsorbents' slow rates of adsorption and their limitations have pushed the scientific community to explore modifications and alternatives.<sup>7–9</sup>

Other methods for the removal of PFAS include electrochemical treatment, <sup>10,11</sup> reverse osmosis treatment, <sup>12</sup> and ion exchange membrane filtration. <sup>13,14</sup> However, these approaches are expensive and have limited effectiveness; as such, the removal of PFAS for large-scale applications remains a persistent challenge. In addition, PFAS removal by adsorption has been increasingly explored using covalent organic frameworks (COF). The high porosity of COFs coupled with their stability at various pH levels makes them favorable adsorbents over high-porosity metal organic frameworks (MOF), particularly at harsh pH levels in aqueous environments. 15,16 The controllable crystallinity of COFs also allows specific arrangement of functional groups to optimize interactions with PFAS surfactants. The efficacy of such frameworks for PFAS adsorption is mainly driven by electrostatic and hydrophobic interactions.16 While they show promising performances with high adsorption rates and for a wide range of PFAS compounds, unfortunately, COFs are typically produced on a small scale and have sensitive syntheses to achieve high crystallinity and, thereby, positional control, which has made this subset of adsorption substrates inaccessible for large-scale PFAS removal.

To overcome these limitations, amorphous porous organic polymers (POP) may be a more cost-effective and easily

Received: September 11, 2022 Accepted: November 17, 2022 Published: December 1, 2022





Scheme 1. Schematic Illustration for the Synthesis of Py-HPOP and Py-TPOP

synthesized alternative to COFs for use as PFAS adsorbents, despite their compromise on two- and three-dimensional spatial arrangement control. For example, Liu et al. have recently developed an amorphous fluorinated triazine-based porous organic polymer that has been successfully used for the reversible adsorption—desorption of PFOA.<sup>17</sup>

To make effective POPs for adsorption, the choice of monomers and moieties is crucial. We have synthesized two separate organic polymers, one using 2,5,8-trichloro-s-heptazine (TCH) and 2,4,6-trichloro-1,3,5-triazine (TCT) as monomers, both cross-linked with 4,4',4",4"'-(pyrene-1,3,6,8tetrayl) tetraaniline (Py-TA) via a nucleophilic substitution approach. Py-TA's amine sites from the aniline groups are available for protonation, which may increase PFOA adsorption. In addition, hydrogen bonding formed between the amine and the carboxylate and/or the fluorinated alkyl chain of PFOA may have a positive effect on the adsorption process. 18,19 This linker is combined with the use of triazine and its derivative, heptazine, to form organic polymers. The synthesis of similar organic polymers using triazine moieties has become well established in recent years due, in part, to their enhancement of thermal stability and surface area.<sup>20–22</sup> Relative to triazine, only recently has heptazine emerged as a building block for porous organic polymer (POP) synthesis.<sup>23</sup> Composed of the  $\pi$ -conjugated system of three triazine fused rings, heptazine linkers offer both enhanced stability as well as higher nitrogen content. 24,25 We used both TCT and TCH to cross-link with Py-TA to enhance the stability of the overall structure and to provide secondary nitrogen groups to facilitate PFOA adsorption. Triazine and triazine-derivatives are susceptible to protonation in the presence of a strong acid such as HCl, making them potential active sites for interaction with PFOA via the electrostatic interactions of the adsorbents' positively charged surface with the anionic head of PFOA.<sup>26</sup>

Therefore, we explored the comparative impact of using heptazine over triazine linkers in the synthesis of two separate POPs, one using 2,5,8-trichloro-s-heptazine and 2,4,6-trichloro-1,3,5-triazine as the monomer, and both are cross-linked with Py-TA (Scheme 1). The polymeric networks we synthesized were explored for their thermal durability, morphological structure, surface area, and their ability to adsorb PFOA in water via batch adsorption experiments under different conditions.<sup>27</sup>

## **■ EXPERIMENTAL SECTION**

Materials. All reagents were used as received. Phosphorus(V) oxychloride (ReagentPlus, 99%), phosphorus pentachloride (reagent grade, 95%), palladium tetrakis(triphenyl phosphine) (99%), potassium carbonate (ReagentPlus, 99%),1,4-dioxane (anhydrous, 99.8%), tetrahydrofuran (THF) (anhydrous, ≥99.9%), and perfluorooctanoic acid (PFOA) (95%) were obtained from Sigma-Aldrich. Cyanuric chloride (>98.0%) and 1,3,6,8-tetrabromopyrene (>98.0%) were obtained from TCI Chemicals. N,N-Diisopropylethylamine (DIPEA) (99.7%) was obtained from Chem-Impex. Melamine (99%) and potassium hydroxide (pellets, certified ACS) were obtained from Fisher Chemical. 4-(4,4,5,5-Tetramethyl-1,3,2-dioxaborolan-2-yl)aniline (98%) was obtained from AmBeed. 4,4',4",4"'-(pyrene-1,3,6,8-tetrayl)tetraaniline (Py-TA) was synthesized according to the referenced procedure.<sup>28</sup> 2,5,8-Trichloro-s-heptazine was synthesized through a modified approach from Luebke et al.;<sup>29</sup> these modifications are described in the SI.

Material Characterization. Fourier transform infrared spectroscopy (FTIR) was carried out using a Shimadzu IRAffinity-1S with a Specac Quest ATR accessory. Nuclear magnetic resonance (NMR) spectroscopy of the intermediates was performed using the Bruker Avance-500. POPs were analyzed by solid-state <sup>13</sup>C NMR (126 MHz) cross-polarization magic angle (CP-MAS) NMR using a Varian Inova-500 at 20 °C using a Phoenix 3.2 mm probe. Thermogravimetric analysis (TGA) was performed using TA Instruments Q500 and platinum sample pans. Nitrogen adsorption isotherms were measured using a Micromeritics 3Flex instrument at 77 K. X-ray diffraction (XRD) was run on a Bruker D8 Advance ECO powder diffractometer

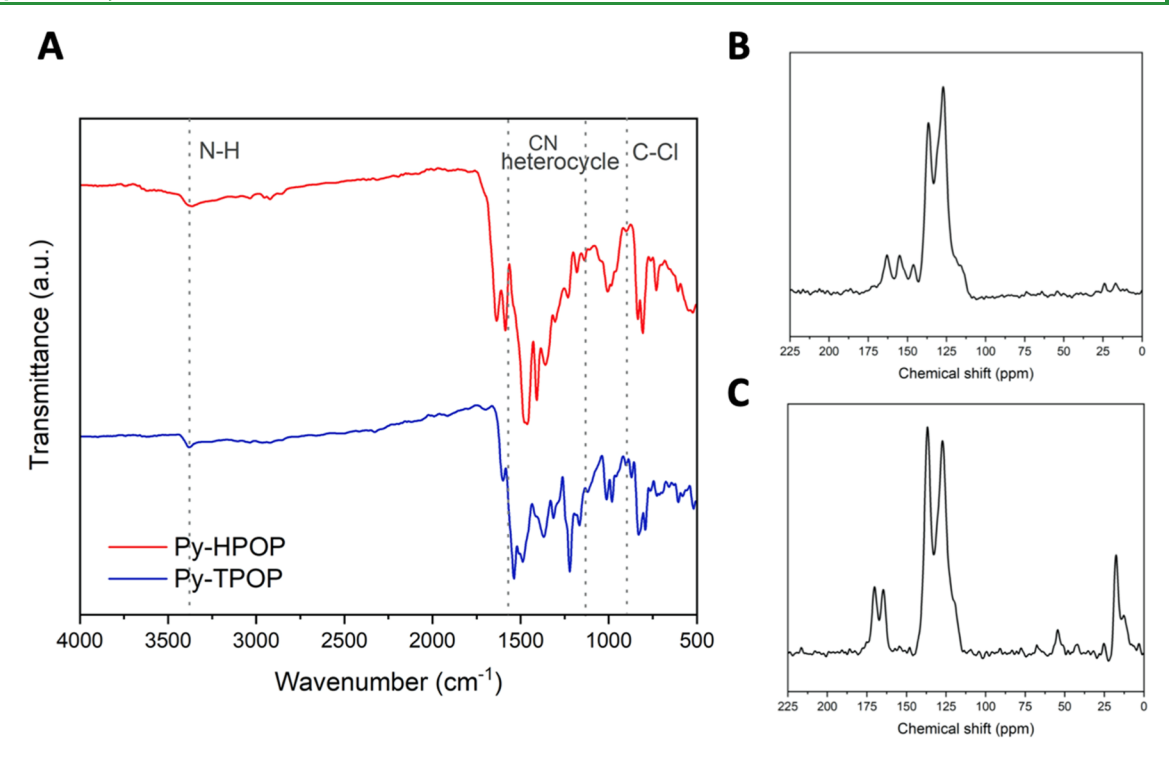


Figure 1. (A) FTIR spectra of Py-HPOP and Py-TPOP powders using ATR-FTIR (B) <sup>13</sup>C CP-MAS NMR of Py-HPOP and (C) Py-TPOP (126 MHz, 20 °C).

and Cu K- $\alpha$  radiation at approximately  $\lambda$  = 1.54 Å, 40 kV and 25 mA. X-ray photoelectron spectroscopy (XPS) was performed using a Scienta Omicron ESCA 2SR instrument at 200 eV pass energy, with the use of a flood gun for charge neutralization due to the nonconductive nature of the samples. Scanning electron microscopy (SEM) was performed using a Zeiss Gemini 500 field emission scanning electron microscope. Particle size distribution (PSD) analysis was performed using a Malvern zetasizer Nanoseries nanozs with triplicates of 5 (10 s) measurements of 0.5 mg mL<sup>-1</sup> samples. Liquid chromatography analysis was performed using a Thermo Electron Finnigan LTO system and a Phenomenex Luna 3 µm-C18 column (100 mm × 4.6 mm). Chromatography run time was 20 min, and the sample injection volume was 10  $\mu$ L. A mobile phase with a flow rate of 0.4 mL min<sup>-1</sup> was composed of 25 mM aqueous ammonium acetate (A) and methanol (B). A gradient was set to 40% solvent B initially, 95% B at 8 min, 50% B at 14 min, and 40% B at 18

Synthesis of Triazine-Based Py-TA Porous Organic Polymer (Py-TPOP). In a 25 mL round bottom flask equipped with a stir bar, Py-TA (56.6 mg, 0.1 mmol) and DIPEA (139.04  $\mu$ L, 0.08 mmol) were dissolved in 4 mL of dry THF and purged with nitrogen for approximately 10 min. The reaction mixture was then cooled in an ice bath and stirred. Once cooled, 2,4,5-trichloro-1,3,5-triazine (24.90 mg, 0.135 mmol) dissolved in 1 mL of THF was added dropwise with stirring. The reaction mixture was stirred at 0 °C for 20 min, followed by an additional 30 min at room temperature, before refluxing overnight. The mixture was then allowed to cool to room temperature before vacuum filtration of the solid using a Buchner funnel, washed with water (2 × 25 mL) and THF (2 × 25 mL) successively. The solid was collected and dried in a vacuum oven at 90 °C. The resulting product was a dark yellow solid (52.9 mg).

Synthesis of Heptazine-Based Py-TA Porous Organic Polymer (Py-HPOP). In a 25 mL round bottom flask equipped with a stir bar, Py-TA (34.0 mg, 0.06 mmol) and 2,5,8-trichloro-s-heptazine (14.8 mg, 0.08 mmol) were dissolved in 4 mL of dry THF, followed by purging with nitrogen for approximately 10 min. The reaction mixture was cooled in an ice bath, followed by the dropwise addition of DIPEA (52.4  $\mu$ L, 0.3 mmol). The reaction mixture was stirred at 0 °C for 30 min, then warmed to room temperature with

stirring for an additional 2 h followed by reflux overnight. The mixture was then allowed to cool to room temperature before vacuum filtration using a Buchner funnel and washed with water and THF successively. The solid was collected and dried in a vacuum oven at 90 °C. The resulting product was a green solid (29.1 mg).

Adsorption Efficiency of PFOA Using Py-HPOP and Py-TPOP. Stock suspensions of 1 mg mL $^{-1}$  concentration of Py-HPOP and Py-TPOP were prepared in 20 mL of MilliQ water and sonicated for 1 h. To prepare the samples, 0.5 mL of one of the stock POP suspensions was added to 2 mL of a 10 mg L $^{-1}$  PFOA solution. This mixture was then diluted with MilliQ water to a final volume of 20 mL, resulting in a final concentration for PFOA of 1 mg L $^{-1}$ . The samples were placed on a rocking shaker for 20 min at room temperature before being passed through a 0.22  $\mu$ m nylon filter and injected into vials, and LC-MS analysis was carried out in triplicate. Further information related to adsorption analysis is available in the SI

Samples diluted with water from Cayuga Lake in the Finger Lakes Region of New York state were prepared in a similar manner. Prior to use, Cayuga lake water was passed through a 0.22  $\mu$ m nylon filter to separate debris and dirt.

Kinetic Study of PFOA Adsorption in Py-HPOP and Py-TPOP. To prepare the samples, 0.5 mL of one of the 1 mg L<sup>-1</sup> stock POP suspensions as prepared above was added to 2 mL of a 10 mg L<sup>-1</sup> PFOA and diluted with 17.5 mL of MilliQ water to reach a final volume of 20 mL. The samples were placed on a rocking shaker while incrementally collecting samples for up to 24 h. All collected samples were passed through a 0.22  $\mu$ m nylon filter and injected into vials, and LC-MS analysis was carried out in triplicate.

Study of Effect of pH on PFOA Adsorption Efficiency. To study the effect of pH on adsorption, 0.5 mL of one of the stock POP suspensions as prepared above was added to 2 mL of a 10 mg L<sup>-1</sup> PFOA solution. This mixture was then diluted with MilliQ water to 20 mL. To this prepared sample, 0.1 M HCl was added dropwise to adjust the pH to 3 by monitoring with a pH meter. Similarly, to prepare a pH 9 sample, 0.1 M NaOH was added dropwise. The samples were placed on a rocking shaker for 20 min, then passed through a 0.22  $\mu$ m nylon filter and injected into vials, and LC-MS analysis was carried out in triplicate.

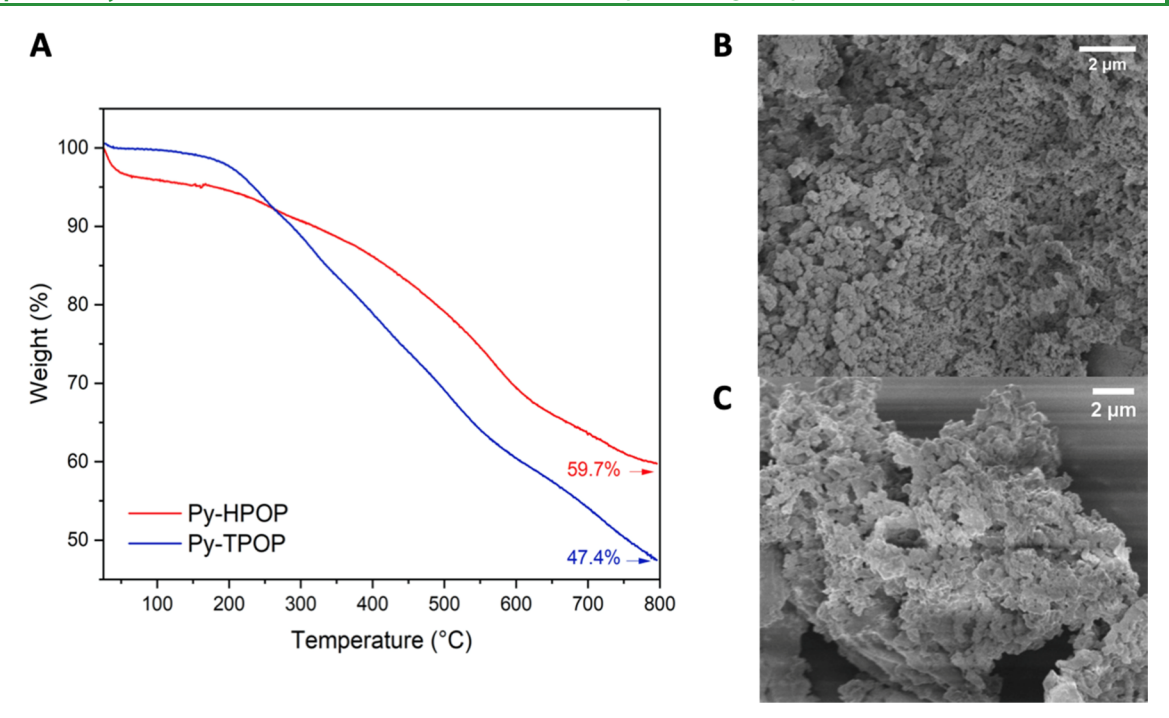


Figure 2. (A) TGA spectra of Py-HPOP and Py-TPOP up to 800 °C, (B) SEM image of Py-HPOP, and (C) SEM image of Py-TPOP.

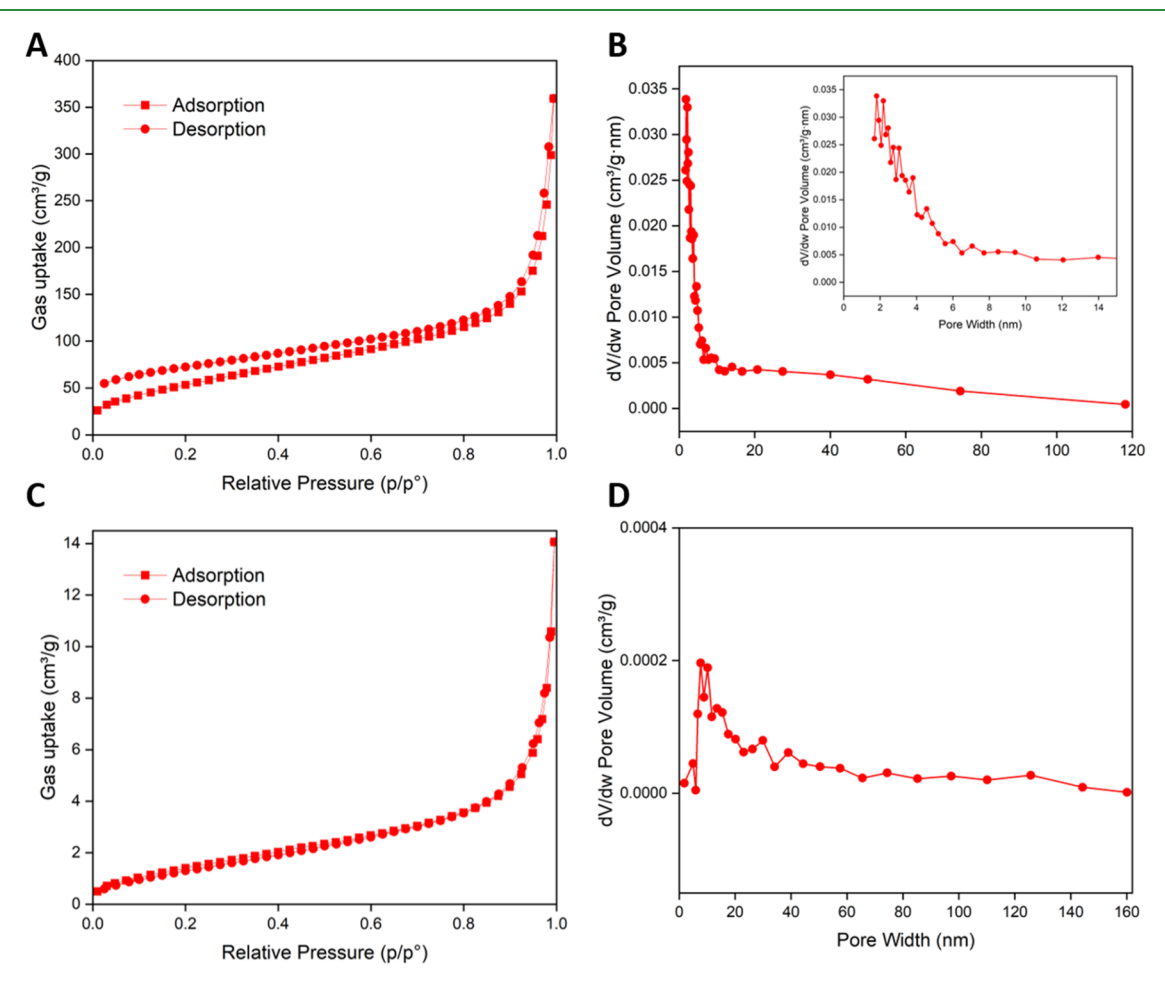


Figure 3. (A) Nitrogen adsorption—desorption isotherm of Py-HPOP; (B) pore size distribution of Py-HPOP; (C) nitrogen adsorption—desorption isotherm of Py-TPOP; and (D) pore size distribution of Py-TPOP. All isotherms were analyzed at 77 K.

## RESULTS AND DISCUSSION

Both Py-TPOP and Py-HPOP were cross-linked by the nucleophilic substitution of Py-TA with TCT and TCH, respectively, both in the presence of DIPEA as a base. The chloride atoms on TCT and TCH are good leaving groups and necessary to ensure a successful synthesis. They are, however, susceptible to hydrolysis upon prolonged exposure to moisture, and therefore the use of anhydrous solvents and nitrogen atmosphere was critical to the reaction. Both POPs were found to be insoluble in water and various organic solvents; this observation is a promising initial indication of network formation, as the degree of cross-linking is inversely linked to solubility.<sup>30</sup>

Structure Characterization of Py-TPOP and Py-HPOP. The N-H stretch associated with the presence of primary amines from the Py-TA aniline groups is observed at 3380 cm<sup>-1</sup> in the FTIR (Figure 1A). Both structures show bands at approximately 1540 and 1585 cm<sup>-1</sup> in Py-TPOP and Py-HPOP, associated with the vibrational stretching of C=N, implying the cross-linking of TCT and TCH to form the resultant polymers. In addition, the peak associated with the C-Cl stretch is almost absent for both POPs, confirming the successful substitutions of TCT and TCH.

The substitution of the heptazine and triazine starting materials for their reactions with Py-TA was confirmed by <sup>13</sup>C CP-MAS NMR spectroscopy (Figure 1B,C). Cross-linking is evident in the absence of the signal originally associated with C–Cl around 175 ppm in Py-HPOP; a signal of minor intensity is visible in Py-TPOP that may be associated with TCT having lower reactivity than TCH.<sup>31</sup> The peaks found at 162.9 and 155.2 ppm, and 170.3 ppm are associated with the heptazine and triazine carbons, respectively.<sup>32,33</sup> Signals observed at the aliphatic region (Figure 1C) are linked to residual DIPEA that was used in the nucleophilic substitution reaction. In addition, a series of peaks ranging from 126.8 to 146.0 ppm indicate the presence of aromatic carbons pertaining to the Py-TA units used in both polymers.<sup>34</sup>

The thermal stabilities of both Py-TPOP and Py-HPOP were analyzed by TGA using a ramp of 10 °C min<sup>-1</sup> under a nitrogen atmosphere. Py-HPOP demonstrates a thermal stability up to approximately 300 °C, compared to Py-TPOP at 200 °C (Figure 2A). The improved stability of Py-HPOP is expected, due to the additional aromaticity afforded by the peripheral nitrogens in the heptazine core. The thermal profile also shows ~4.00% weight loss in Py-HPOP initially between 25 and 100 °C, which we have attributed to the release of trapped solvents in the structure. This low-temperature weight loss was less pronounced in Py-TPOP; we hypothesize this is due to both a lower surface area and lower inherent porosity of Py-TPOP, resulting in less solvent entrapment.

The SEM images, obtained to visually probe the morphology of both polymers, show that both Py-TPOP and Py-HPOP have irregular-shaped aggregate morphologies with porous characteristics (Figure 2B,C). However, Py-HPOP showed a significantly more textured, spherical morphology compared to Py-TPOP. Despite this difference, particle size distribution results point toward Py-TPOP and Py-HPOP having similar sizes, with an average diameter at 1176 versus 1118 nm for Py-TPOP and Py-HPOP, respectively (Figure S7). Therefore, the morphological variation between both POPs may be due to the more structurally rigid fused ring system of heptazine that

prevents the pores from collapsing under vacuum. Both demonstrate an irregularity in shape, most likely connected to the absence of any long-range order within both structures, resulting in both being amorphous polymers, as observed in the XRD analysis (Figure S2).

The porosity of both polymers was investigated through a nitrogen adsorption—desorption isotherm, performed at 77 K. The nitrogen ( $N_2$ ) isotherms of Py-HPOP display a type II reversible adsorption (Figure 3A). This isotherm pattern is indicative of mesopores (2–50 nm diameter), characterized by monolayer adsorption at lower relative pressure (0–0.2  $p/p_0$  range), followed by multilayer adsorption (0.2–0.8  $p/p_0$  range) before  $N_2$  condensation occurs in the pores.<sup>39,40</sup> Conversely, the nitrogen isotherm from Py-TPOP shows a lower surface area.

The pore size distribution (PSD) (Figure 3B) of Py-HPOP supports our conclusion regarding the mesoporous nature of the structure, given the majority of pore size widths were found to be less than 15 nm, with a cumulative pore volume of of 0.57 cm³ g⁻¹ for Py-HPOP and merely 0.02 cm³ g⁻¹ for Py-TPOP. As such, the Brunauer–Emmett–Teller (BET) surface areas ( $S_{\rm BET}$ ) of Py-HPOP and Py-TPOP were found to be drastically different at 205.2 and 4.6 m² g⁻¹, respectively. Examples of  $S_{\rm BET}$  for other amorphous heptazine-based organic polymers in the literature range from 115.8 to 424 m² g⁻¹. <sup>41,42</sup> Conversely, the low  $S_{\rm BET}$  of Py-TPOP may be a result of its higher framework flexibility that is eliminated when switching to rigid heptazine linkers.

Adsorption of PFOA by Py-HPOP and Py-TPOP. To study the adsorption capabilities of both POPs for the removal of PFOA, 0.5 mg of the polymers were used to treat a 1 mg  $L^{-1}$ aqueous solution of PFOA for 20 min. By measuring the free PFOA content in the aqueous samples using LC-MS after treatment, PFOA removal percentage via Py-HPOP was found to be 80.8 versus 98.4% for Py-TPOP. While this experiment demonstrates the capabilities of both polymers toward the adsorption of PFOA, Py-TPOP outperformed Py-HPOP for PFOA removal despite Py-TPOP's inferior nonporous  $S_{\text{BET}}$ . This phenomenon has previously been reported in the literature. 43 We suggest that, despite Py-HPOP's high S<sub>BET</sub>, its high degree of cross-linking may contribute to steric hindrance, which reduces access to adsorption sites lowering PFOA removal. Comparing to other studies using various amounts of adsorbing materials with an initial PFOA concentration at 1 mg  $\rm L^{-1}$ , Py-TPOP particularly demonstrates competitive performance compared to aluminum-based water treatment residuals at 97.4% removal and multiwalled carbon nanotubes with electrochemical assistance at 92% removal. 44,45

The kinetics of PFOA adsorption were also compared for both POPs to determine the optimal treatment period. Both adsorbents exhibited fast adsorption kinetics common for adsorption processes facilitated by electrostatic interactions, with the maximum adsorption achieved in less than 1 h. While this treatment time is promising for efficient PFOA removal, POPs have been reported that can achieve 99.99% removal in 2 min. An Nonetheless, our synthesis is advantageous as it can facilitate future performance improvements through surface tuning. PFOA adsorption via both POPs showed pseudosecond-order kinetics (SI, eq 6). R2 was 0.9995 and 0.9992, for Py-HPOP and Py-TPOP, respectively. More specifically, this time-dependent adsorption trend of PFOA can be explained by the availability of the functional groups in the POPs to serve as adsorption sites during the treatment. Initially, more

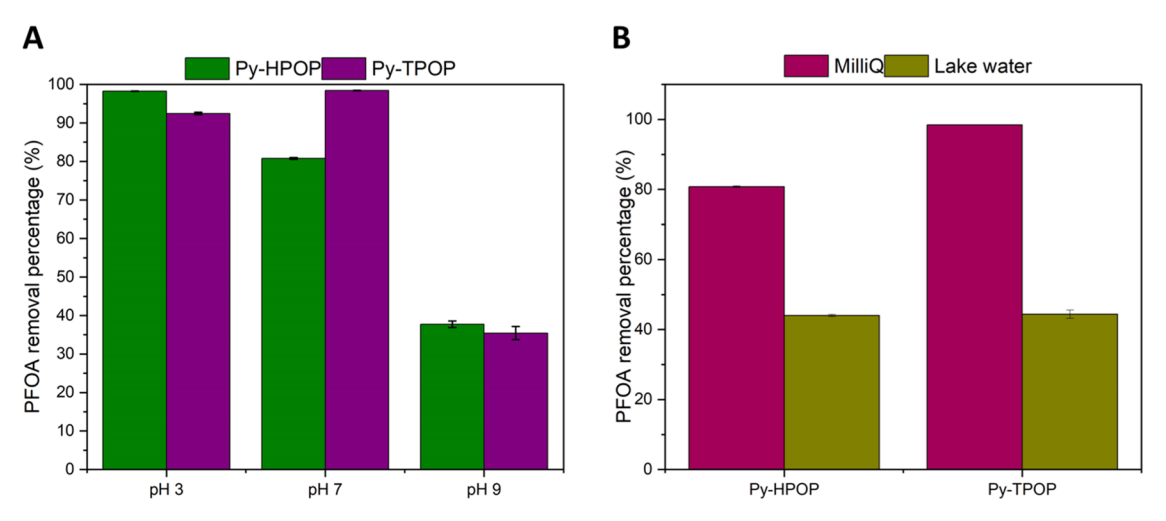


Figure 4. (A) PFOA removal percentage by change in pH. (B) PFOA removal percentage by change in MilliQ and Cayuga lake water.

adsorption sites are freely available for interaction with PFOA; as these sites are further occupied, the remaining sites become more encumbered, resulting in higher solute-solute interactions such as repulsion interactions and weak hydrophobic interactions. This elucidates the hysteretic adsorption observed (Figure S9) with some desorption occurring with further treatment time. The  $k_2$  adsorption rate constant was found to be 5.3 g mg $^{-1}$  h $^{-1}$  for Py-HPOP and 450.3 g mg $^{-1}$  h $^{-1}$  for Py-TPOP, exhibiting Py-TPOP as a faster adsorbent in the removal of PFOA.

Experiments were conducted to explore the effect of pH on the underlying interactions behind the adsorption of PFOA and our polymers. In various samples using Py-HPOP at pH 3, 7, and 9, minimal adsorption was achieved in basic conditions (Figure 4A). Treatments using Py-TPOP show a similar trend. This pH-dependence of PFOA adsorption may be linked to adsorbent surface charge properties, which were explored via a point of zero charge (PZC) study (Figure S13). The pH<sub>PZC</sub> values are found at approximately pH 7.7 and pH 6.9 for Py-HPOP and Py-TPOP, respectively. This indicates that both POPs have a negative surface charge during the pH 9 treatments, as pH > pH<sub>PZC</sub>. By increasing the pH, the electrostatic interactions of the adsorbing substrates with PFAS are reduced due to the decrease in positive surface charge of the POPs with the anionic head of PFOA, as well as possible electrostatic repulsion interactions such as in the presence of hydroxide anionic species. 48 Because the experimental pH ranges exceeded PFOA's  $pK_a$ , PFOA is predominantly present in the conjugate base form. Therefore, the pH study shows that, by tuning the POP adsorbent surface charge by pH, the interactions of the negatively charged PFOA with the POPs can be optimized to increase electrostatic interactions and adsorption of PFOA as a result.47

This phenomenon is also demonstrated in treatments carried out using lake water instead of MilliQ water. The primary objective of this experiment was to simulate the effect of using the POPs for the treatment of natural drinking water sources such as Cayuga Lake, one of New York State's Finger Lakes located in Ithaca, NY. The decline in PFOA removal in lake water compared to MilliQ water was unsurprising due to Cayuga Lake's unusually high-mineral content. It is probable that competitive electrostatic interactions with the adsorbing substrates may create charge screening or even interaction with the adsorbent surfaces, which result in lower PFOA removal

rates. <sup>49,50</sup> The reduced adsorption in natural water samples confirm that the predominant adsorption mechanism of PFOA by these polymers is due to electrostatic interactions.

#### CONCLUSION

In summary, we have developed triazine- and heptazineenriched POPs via a one-pot nucleophilic substitution approach. Py-HPOP showed superior physical properties over Py-TPOP, such as higher  $S_{\rm BET}$  at 205.2 m<sup>2</sup> g<sup>-1</sup> and a thermal stability to approximately 300 °C. Despite this, Py-TPOP was shown to be more effective in PFOA adsorption, at 98.4% removal, by way of electrostatic interactions, favoring pH below the pH $_{PZC}$ . Testing both POPs for the adsorption in lake water suggests that other minerals in water may cause competitive electrostatic interactions, thereby hindering PFOA adsorption. Future work would focus on optimization of conditions for effective PFOA adsorption and reversible desorption in water. Overall, the study of these POPs, especially Py-TPOP, is encouraging to the future exploration of amorphous, low BET surface area materials for practical PFOA removal applications.

### ASSOCIATED CONTENT

# Supporting Information

The Supporting Information is available free of charge at https://pubs.acs.org/doi/10.1021/acsapm.2c01580.

Additional detailed experimental data including: Methodology of the synthesis of TCH, <sup>1</sup>H and <sup>13</sup>C NMR of starting materials, FTIR of starting materials, XRD, XPS, PZC studies and particle size distribution spectra of Py-TPOP and Py-HPOP, and PFOA adsorption analysis (PDF)

## AUTHOR INFORMATION

## **Corresponding Author**

Alireza Abbaspourrad — Food Science Department, College of Agriculture and Life Sciences, Cornell University, Ithaca, New York 14853, United States; orcid.org/0000-0001-5617-9220; Email: alireza@cornell.edu

#### Authors

Dana Abdullatif – Department of Chemistry and Chemical Biology, Cornell University, Ithaca, New York 14853, United

- States; Food Science Department, College of Agriculture and Life Sciences, Cornell University, Ithaca, New York 14853, United States; occid.org/0000-0001-7390-9408
- Ahmadreza Khosropour Food Science Department, College of Agriculture and Life Sciences, Cornell University, Ithaca, New York 14853, United States
- Anahita Khojastegi Food Science Department, College of Agriculture and Life Sciences, Cornell University, Ithaca, New York 14853, United States
- Imann Mosleh Food Science Department, College of Agriculture and Life Sciences, Cornell University, Ithaca, New York 14853, United States; ⊙ orcid.org/0000-0001-8763-6906
- Leila Khazdooz Food Science Department, College of Agriculture and Life Sciences, Cornell University, Ithaca, New York 14853, United States
- Amin Zarei Food Science Department, College of Agriculture and Life Sciences, Cornell University, Ithaca, New York 14853, United States

Complete contact information is available at: https://pubs.acs.org/10.1021/acsapm.2c01580

## **Author Contributions**

D.A.: Conceptualization, investigation, methodology, validation, data curation, writing- original draft, writing-reviewing & editing A.K.: Conceptualization, methodology, investigation, supervision, writing- reviewer & editing A.K.: Investigation I.M.: Investigation A.Z.: Methodology A.A.: Conceptualization, funding acquisition, supervision, resources, writing-reviewing & editing.

#### **Funding**

This work made use of the Cornell Center for Materials Research Shared Facilities which are supported through the NSF MRSEC program (DMR-1719875). This work also made use of the Cornell University NMR Facility, which is supported, in part, by the NSF through MRI award CHE-1531632.

#### **Notes**

The authors declare no competing financial interest.

## ACKNOWLEDGMENTS

The authors thank Kelley J. Donaghy for her insight during this project, and Ivan Keresztes for his technical support at the Cornell University NMR Facility.

# REFERENCES

- (1) Bolan, N.; Sarkar, B.; Yan, Y.; Li, Q.; Wijesekara, H.; Kannan, K.; Tsang, D. C. W.; Schauerte, M.; Bosch, J.; Noll, H.; Ok, Y. S.; Scheckel, K.; Kumpiene, J.; Gobindlal, K.; Kah, M.; Sperry, J.; Kirkham, M. B.; Wang, H.; Tsang, Y. F.; Hou, D.; Rinklebe, J. Remediation of Poly- and Perfluoroalkyl Substances (PFAS) Contaminated Soils To Mobilize or to Immobilize or to Degrade? *J. Hazard. Mater.* 2021, 401, No. 123892.
- (2) Glüge, J.; Scheringer, M.; Cousins, I. T.; DeWitt, J. C.; Goldenman, G.; Herzke, D.; Lohmann, R.; Ng, C. A.; Trier, X.; Wang, Z. An Overview of the Uses of per- and Polyfluoroalkyl Substances (PFAS). *Environ. Sci.: Processes Impacts* **2020**, 22, 2345–2373.
- (3) Gagliano, E.; Sgroi, M.; Falciglia, P. P.; Vagliasindi, F. G. A.; Roccaro, P. Removal of Poly- and Perfluoroalkyl Substances (PFAS) from Water by Adsorption: Role of PFAS Chain Length, Effect of Organic Matter and Challenges in Adsorbent Regeneration. *Water Res.* 2020, 171, No. 115381.

- (4) Kancharla, S.; Alexandridis, P.; Tsianou, M. Sequestration of perand Polyfluoroalkyl Substances (PFAS) by Adsorption: Surfactant and Surface Aspects. *Curr. Opin. Colloid Interface Sci.* **2022**, *58*, No. 101571.
- (5) Domingo, J. L.; Nadal, M. Human Exposure to per- and Polyfluoroalkyl Substances (PFAS) through Drinking Water: A Review of the Recent Scientific Literature. *Environ. Res.* **2019**, *177*, No. 108648.
- (6) Steenland, K.; Fletcher, T.; Savitz, D. A. Epidemiologic Evidence on the Health Effects of Perfluorooctanoic Acid (PFOA). *Environ. Health Perspect.* **2010**, *118*, 1100–1108.
- (7) Wang, Y.; Darling, S. B.; Chen, J. Selectivity of Per- and Polyfluoroalkyl Substance Sensors and Sorbents in Water. *ACS Appl. Mater. Interfaces* **2021**, *13*, 60789–60814.
- (8) Xu, J.; Liu, Z.; Zhao, D.; Gao, N.; Fu, X. Enhanced Adsorption of Perfluorooctanoic Acid (PFOA) from Water by Granular Activated Carbon Supported Magnetite Nanoparticles. *Sci. Total Environ.* **2020**, 723, No. 137757.
- (9) Saleh, T. A. Nanomaterials: Classification, Properties, and Environmental Toxicities. *Environ. Technol. Innovation* **2020**, 20, No. 101067.
- (10) Lin, H.; Wang, Y.; Niu, J.; Yue, Z.; Huang, Q. Efficient Sorption and Removal of Perfluoroalkyl Acids (PFAAs) from Aqueous Solution by Metal Hydroxides Generated in Situ by Electrocoagulation. *Environ. Sci. Technol.* **2015**, 49, 10562–10569.
- (11) Schaefer, C. E.; Tran, D.; Fang, Y.; Choi, Y. J.; Higgins, C. P.; Strathmann, T. J. Electrochemical Treatment of Polyand Perfluoroalkyl Substances in Brines. *Environ. Sci.: Water Res. Technol.* **2020**, *6*, 2704–2712.
- (12) Flores, C.; Ventura, F.; Martin-Alonso, J.; Caixach, J. Occurrence of Perfluorooctane Sulfonate (PFOS) and Perfluorooctanoate (PFOA) in N.E. Spanish Surface Waters and Their Removal in a Drinking Water Treatment Plant That Combines Conventional and Advanced Treatments in Parallel Lines. *Sci. Total Environ.* **2013**, 461–462, 618–626.
- (13) Zaggia, A.; Conte, L.; Falletti, L.; Fant, M.; Chiorboli, A. Use of Strong Anion Exchange Resins for the Removal of Perfluoroalkylated Substances from Contaminated Drinking Water in Batch and Continuous Pilot Plants. *Water Res.* **2016**, *91*, 137–146.
- (14) Liu, Y.-L.; Sun, M. Ion Exchange Removal and Resin Regeneration to Treat per- and Polyfluoroalkyl Ether Acids and Other Emerging PFAS in Drinking Water. *Water Res.* **2021**, 207, No. 117781.
- (15) Ji, W.; Xiao, L.; Ling, Y.; Ching, C.; Matsumoto, M.; Bisbey, R. P.; Helbling, D. E.; Dichtel, W. R. Removal of GenX and Perfluorinated Alkyl Substances from Water by Amine-Functionalized Covalent Organic Frameworks. *J. Am. Chem. Soc.* **2018**, *140*, 12677—12681.
- (16) Wang, W.; Zhou, Z.; Shao, H.; Zhou, S.; Yu, G.; Deng, S. Cationic Covalent Organic Framework for Efficient Removal of PFOA Substitutes from Aqueous Solution. *Chem. Eng. J.* **2021**, *412*, No. 127509.
- (17) Liu, G.; Wei, X.; Luo, P.; Dai, S.; Zhang, W.; Zhang, Y. Novel Fluorinated Nitrogen-Rich Porous Organic Polymer for Efficient Removal of Perfluorooctanoic Acid from Water. *Water* **2022**, *14*, No. 1010.
- (18) Mei, W.; Sun, H.; Song, M.; Jiang, L.; Li, Y.; Lu, W.; Ying, G.-G.; Luo, C.; Zhang, G. Per- and Polyfluoroalkyl Substances (PFASs) in the Soil-Plant System: Sorption, Root Uptake, and Translocation. *Environ. Int.* **2021**, *156*, No. 106642.
- (19) Wang, M.; Orr, A. A.; Jakubowski, J. M.; Bird, K. E.; Casey, C. M.; Hearon, S. E.; Tamamis, P.; Phillips, T. D. Enhanced Adsorption of per- and Polyfluoroalkyl Substances (PFAS) by Edible, Nutrient-Amended Montmorillonite Clays. *Water Res.* **2021**, *188*, No. 116534.
- (20) Liu, M.; Guo, L.; Jin, S.; Tan, B. Covalent Triazine Frameworks: Synthesis and Applications. *J. Mater. Chem. A* **2019**, *7*, 5153–5172.
- (21) Zhang, Y.; Hong, X.; Cao, X.-M.; Huang, X.-Q.; Hu, B.; Ding, S.-Y.; Lin, H. Functional Porous Organic Polymers with Conjugated

- Triaryl Triazine as the Core for Superfast Adsorption Removal of Organic Dyes. ACS Appl. Mater. Interfaces 2021, 13, 6359-6366.
- (22) Wang, B.; Lee, L. S.; Wei, C.; Fu, H.; Zheng, S.; Xu, Z.; Zhu, D. Covalent Triazine-Based Framework: A Promising Adsorbent for Removal of Perfluoroalkyl Acids from Aqueous Solution. *Environ. Pollut.* **2016**, 216, 884–892.
- (23) Ehrmaier, J.; Rabe, E. J.; Pristash, S. R.; Corp, K. L.; Schlenker, C. W.; Sobolewski, A. L.; Domcke, W. Singlet-Triplet Inversion in Heptazine and in Polymeric Carbon Nitrides. *J. Phys. Chem. A* **2019**, 123, 8099–8108.
- (24) Holst, J. R.; Gillan, E. G. From Triazines to Heptazines: Deciphering the Local Structure of Amorphous Nitrogen-Rich Carbon Nitride Materials. *J. Am. Chem. Soc.* **2008**, *130*, 7373–7379.
- (25) Zhang, J.; Shi, J.; Cui, Z.; Chu, S.; Wang, Y.; Zou, Z. Highly Efficient Hydrogen Evolution from Water Splitting on Heptazine Polymer with Three Types of Defects. *Appl. Surf. Sci.* **2022**, *580*, No. 152070.
- (26) Guerrini, M.; Aznar, E. D.; Cocchi, C. Electronic and Optical Properties of Protonated Triazine Derivatives. *J. Phys. Chem. C* **2020**, 124, 27801–27810.
- (27) Saleh, T. A. Protocols for synthesis of nanomaterials, polymers, and green materials as adsorbents for water treatment technologies. *Environ. Technol. Innovation* **2021**, 24, No. 101821.
- (28) Mosleh, I.; Khosropour, A. R.; Aljewari, H.; Carbrello, C.; Qian, X.; Wickramasinghe, R.; Abbaspourrad, A.; Beitle, R. Cationic Covalent Organic Framework as an Ion Exchange Material for Efficient Adsorptive Separation of Biomolecules. ACS Appl. Mater. Interfaces 2021, 13, 35019–35025.
- (29) Luebke, R.; Weseliński, ŁJ.; Belmabkhout, Y.; Chen, Z.; Wojtas, Ł.; Eddaoudi, M. Microporous Heptazine Functionalized (3,24)-Connected Rht-Metal—Organic Framework: Synthesis, Structure, and Gas Sorption Analysis. *Cryst. Growth Des.* **2014**, *14*, 414–418.
- (30) Nie, W.; Liu, J.; Bai, X.; Xing, Z.; Gao, Y. Designing Phenyl Porous Organic Polymers with High-Efficiency Tetracycline Adsorption Capacity and Wide pH Adaptability. *Polymers* **2022**, *14*, No. 203.
- (31) Sharma, N.; Kumar, S.; Battula, V. R.; Kumari, A.; Giri, A.; Patra, A.; Kailasam, K. A Tailored Heptazine-Based Porous Polymeric Network as a Versatile Heterogeneous (Photo)catalyst. *Chem. Eur. J.* **2021**, *27*, 10649–10656.
- (32) Xu, C.; Qian, L.; Lin, J.; Guo, Z.; Yan, D.; Zhan, H. Heptazine-Based Porous Polymer for Selective CO2 Sorption and Visible Light Photocatalytic Oxidation of Benzyl Alcohol. *Microporous Mesoporous Mater.* **2019**, 282, 9–14.
- (33) Kumar, S.; et al. Triazine Based Nanoarchitectonics of Porous Organic Polymers for CO2 Storage. *Mater. Lett.* **2022**, 313, No. 131757.
- (34) Wang, S.; Sun, Q.; Chen, W.; Tang, W.; Aguila, B.; Pan, Y.; Zheng, A.; Yang, Z.; Wojtas, L.; Ma, S.; Xiao, F-S. Programming Covalent Organic Frameworks for Photocatalysis: Investigation of Chemical and Structural Variations. *Matter* **2020**, *2*, 416–427.
- (35) Yang, J.; Gong, X.; Wang, G. Structure, Aromaticity, Stability, and Energetic Performance of the Analogues and Derivatives of S-Heptazine. *J. Mol. Model.* **2014**, *20*, No. 2379.
- (36) Chamorro-Posada, P.; Dante, R. C.; Vázquez-Cabo, J.; Dante, D. G.; Martín-Ramos, P.; Rubiños-López, Ó.; Sánchez-Arévalo, F. M. Experimental and Theoretical Investigations on a CVD Grown Thin Film of Polymeric Carbon Nitride and Its Structure. *Diamond Relat. Mater.* **2021**, *111*, No. 108169.
- (37) Rossman, M. A.; Leonard, N. J.; Urano, S.; LeBreton, P. R. Synthesis and Valence Orbital Structures of azacycl[3.3.3]azines in a Systematic Series. *J. Am. Chem. Soc.* **1985**, *107*, 3884–3890.
- (38) Jiao, S.; Deng, L.; Zhang, X.; Zhang, Y.; Liu, K.; Li, S.; Wang, L.; Ma, D. Evaluation of an Ionic Porous Organic Polymer for Water Remediation. *ACS Appl. Mater. Interfaces* **2021**, *13*, 39404–39413.
- (39) Thommes, M.; Kaneko, K.; Neimark, A. V.; Olivier, J. P.; Rodriguez-Reinoso, F.; Rouquerol, J.; Sing, K. S. W. Physisorption of Gases, With Special Reference to the Evaluation of Surface Area and Pore Size Distribution (IUPAC Technical Report). *Pure Appl. Chem.* **2015**, *87*, 1051–1069.

- (40) Arab, P.; Rabbani, M. G.; Sekizkardes, A. K.; İslamoğlu, T.; El-Kaderi, H. M. Copper(I)-Catalyzed Synthesis of Nanoporous Azo-Linked Polymers: Impact of Textural Properties on Gas Storage and Selective Carbon Dioxide Capture. *Chem. Mater.* **2014**, *26*, 1385–1392
- (41) Dang, Q.-Q.; Zhan, Y.-F.; Wang, X.-M.; Zhang, X.-M. Heptazine-Based Porous Framework for Selective CO2 Sorption and Organocatalytic Performances. *ACS Appl. Mater. Interfaces* **2015**, 7, 28452–28458.
- (42) Sharma, N.; Ugale, B.; Kumar, S.; Kailasam, K. Metal-Free Heptazine-Based Porous Polymeric Network as Highly Efficient Catalyst for CO Capture and Conversion. *Front Chem* **2021**, *9*, No. 737511.
- (43) Xiao, L.; Ling, Y.; Alsbaiee, A.; Li, C.; Helbling, D. E.; Dichtel, W. R.  $\beta$ -Cyclodextrin Polymer Network Sequesters Perfluorooctanoic Acid at Environmentally Relevant Concentrations. *J. Am. Chem. Soc.* **2017**, 139, 7689–7692.
- (44) Zhang, Z.; Sarkar, D.; Datta, R.; Deng, Y. Adsorption of perfluorooctanoic acid (PFOA) and perfluorooctanesulfonic acid (PFOS) by aluminum-based drinking water treatment residuals. *J. Hazard. Mater. Lett.* **2021**, *2*, No. 100034.
- (45) Li, X.; Chen, S.; Quan, X.; Zhang, Y. Enhanced Adsorption of PFOA and PFOS on Multiwalled Carbon Nanotubes under Electrochemical Assistance. *Environ. Sci. Technol.* **2011**, *45*, 8498–8505.
- (46) Liu, X.; Zhu, C.; Yin, J.; Li, J.; Zhang, Z.; Li, J.; Shui, F.; You, Z.; Shi, Z.; Li, B.; Bu, X.-H.; Nafady, A.; Ma, S. Installation of Synergistic Binding Sites onto Porous Organic Polymers for Efficient Removal of Perfluorooctanoic Acid. *Nat. Commun.* **2022**, *13*, No. 2132.
- (47) Hussain, F. A.; Janisse, S. E.; Heffern, M. C.; Kinyua, M.; Velázquez, J. M. Adsorption of Perfluorooctanoic Acid from Water by pH-Modulated Brönsted Acid and Base Sites in Mesoporous Hafnium Oxide Ceramics. *iScience* **2022**, 25, No. 104138.
- (48) Wang, F.; Shih, K. Adsorption of Perfluorooctanesulfonate (PFOS) and Perfluorooctanoate (PFOA) on Alumina: Influence of Solution pH and Cations. *Water Res.* **2011**, *45*, 2925–2930.
- (49) Wang, F.; Liu, C.; Shih, K. Adsorption Behavior of Perfluorooctanesulfonate (PFOS) and Perfluorooctanoate (PFOA) on Boehmite. *Chemosphere* **2012**, *89*, 1009–1014.
- (50) Wing, M. R.; Preston, A.; Acquisto, N.; Ahrnsbrak, W. F. Intrusion of Saline Groundwater into Seneca and Cayuga Lakes, New York. *Limnol. Oceanogr.* **1995**, *40*, 791–801.